

Thermal Degradation Kinetic Study of a Fuel-rich Energetic Mixture Containing Epoxy Binder

M.R. Sovizi*, G. Fakhropour and A.R. Madram

Department of Chemistry, Malek Ashtar University of Technology, P.O. Box: 16765-3454, Tehran, Iran

(Received 28 February 2016, Accepted 17 April 2016)

In this work, thermal degradation behavior of a fuel-rich energetic mixture containing epoxy binder was studied by thermogravimetric analysis and differential scanning calorimetry under dynamic nitrogen atmosphere at different heating rates. Variation of the thermal degradation activation energy of the mixture was evaluated by differential and integral isoconversional methods *via* AKTS software package. Model fitting methods were used to determine the reaction model and pre-exponential factor of thermal degradation of the energetic mixture. Verification of the thermal degradation reaction model was done by differential master-plot method. The calculated values of $\ln A$ and E_a of the energetic mixture, according to Kissinger method, were 23.9 s^{-1} and 155 kJ mol^{-1} , respectively. Self-accelerating decomposition temperature and explosion critical temperature of the energetic mixture were determined to evaluate the thermal stability.

Keywords: Fuel-rich, Kinetic thermal degradation, Energetic mixture, Epoxy, AKTS software

INTRODUCTION

The energetic mixtures containing high content of metal fuels are so called metal fuel-rich mixtures. Aluminum, magnesium and aluminum-magnesium alloys are widely used as fuels in energetic mixtures such as pyrotechnics, explosives and propellants [1]. Due to the reaction of water as an oxidizing agent and metals as a fuel, and production of hydrogen during an exothermic reaction, these combinations were introduced as a green underwater propellant system. These systems are also called hydro-reactive propulsive systems [2].

Metallic powders can be mixed with common solid oxidizers to produce propellant systems. Ammonium perchlorate (AP) is an ideal oxidizer for solid composite propellants, because it is decomposed into fully gaseous products [3,4]. Ingredients of a propellant can be fixed by a polymeric binder such as hydroxyl terminated poly

(butadiene) (HTPB), carboxy terminated poly(butadiene) (CTPB), and epoxy resin [3]. Wang Q. *et al.* studied the kinetic and thermodynamic parameters of a nitrated HTPB (NHTPB) sample by DSC measurement at different heating rates, and compared its thermal behavior with HTPB samples [5]. Thermal properties of a Mg-based fuel-rich propellant containing HTPB/AP/Mg/Additive (12/20/65/3) used for water ramjet engines were characterized by differential thermal analysis (DTA) and simultaneous thermogravimetry (TG) [6]. Sippel T.R. *et al.* [7] investigated aluminum agglomeration reduction in a composite propellant containing Al/AP/HTPB, as a composite solid propellant, using tailored Al/PTFE (polytetrafluoroethylene) particles. Ghassemi H. and Farshi Fasih H. [8] investigated the propulsive characteristics of metal fuels in a hydro-combustion chamber in a thermodynamic approach. They studied thermochemistry of common metal fuels and water having magnesium, using chemical equilibrium calculations.

Thermal analysis study of energetic materials is

*Corresponding author. E-mail: mrsovizi@mut.ac.ir

important to understand the thermal decomposition kinetics as well as the effect of exothermic decomposition reaction of these materials on the potential danger in their processing, usage and storage [9,10]. We can obtain useful information about thermal stability and lifetime of energetic materials by kinetic analyses [11]. A reliable evaluation of the kinetic parameters allowing theoretical explanation of the experimental data and supplies a mathematical description to extrapolate its behavior in different conditions.

In spite of investigation about thermal behavior of the fuel-rich energetic materials, few kinetic studies have been reported [1,12], and there is not any information about thermal degradation kinetic parameters of the fuel-rich energetic mixture containing epoxy binder. Therefore, this study was undertaken to investigate the non-isothermal degradation of an energetic mixture containing Mg-Al/AP/Strontium nitrate/Epoxy using DSC/TGA under nitrogen atmosphere. The variation of degradation activation energy with degree of conversion (α) was evaluated by Kissinger-Akahira-Sunose (KAS), Flynn-Wall-Ozawa (FWO), Friedman's isoconversional methods (FR) and by AKTS Thermokinetics software package [13]. Model fitting methods were also used to determine the triplet kinetic parameters. Differential master-plot method was also used to verify the degradation reaction mechanism. Self-accelerating decomposition temperature (T_{SADT}) and explosion critical temperature (T_b) of the energetic mixture were determined to evaluate the thermal stability. The results of this study will provide a useful information for applications of metal fuel-rich as a hydro-reactive propulsion system.

THEORETICAL APPROACH

Solid State Kinetics

Thermal degradation reaction rate can usually be expressed as [14]:

$$\frac{d\alpha}{dt} = k(T) f(\alpha) \quad (1)$$

where T is absolute temperature (given in Kelvin), α the degree of conversion, $f(\alpha)$ differential reaction model

function (a list of common reaction models is shown in Table 1 [15]), and $k(T)$ is reaction rate constant which follows the Arrhenius law:

$$k(T) = A \exp\left(-\frac{E_a}{RT}\right) \quad (2)$$

where A is pre-exponential or frequency factor, E_a is activation energy and R is universal gas constant [expressed in units of $\text{kJ mol}^{-1} \text{K}^{-1}$].

The differential form of non-isothermal rate law [16], at a constant heating rate ($\beta = dT/dt$), can be written as:

$$\frac{d\alpha}{dt} = \frac{A}{\beta} \exp\left(-\frac{E_a}{RT}\right) f(\alpha) \quad (3)$$

where, t is time, and da/dT is non-isothermal reaction rate, which is equal to $(1/\beta) da/dt$.

Model-free Methods

Arrhenius parameters can be determined by model-free methods without assuming any specific reaction models [16]. Several isoconversional methods are developed to obtain variation of the activation energy as a function extent of conversion. Friedman method [17] is a differential isoconversional method based on the Eq. (3) in logarithmic form and leads to:

$$\ln\left[\beta_i \left(\frac{d\alpha}{dT}\right)_{\alpha,i}\right] = \ln[A_\alpha f(\alpha)_i] - \frac{E_{a,\alpha}}{RT_{\alpha,i}} \quad (4)$$

where subscripts α and i assign a given value of extent of conversion and heating rate, respectively. The activation energy values can be determined by plotting $\ln[\beta(da/dT)]$ against $1/T$ at each α obtained from curves recorded at several heating rates.

Flynn-Wall-Ozawa method (FWO) is an integral isoconversional calculation method [18,19] based on Doyle's approximation of temperature integral with the following equation:

$$\log \beta = \log \frac{AE_a}{Rg(\alpha)} - 2.315 - 0.4567 \frac{E_a}{RT} \quad (5)$$

A linear plot of $\ln\beta$ vs. $1/T$ at each α yields E_a from the slope

Table 1. Some Common Kinetic Reaction Models

No.	Symbol	reaction model	$f(\alpha)$	$g(\alpha)$
1	P1	Power law	$4\alpha^{3/4}$	$\alpha^{1/4}$
2	P2	Power law	$3\alpha^{2/3}$	$\alpha^{1/3}$
3	P3	Power law	$2\alpha^{1/2}$	$\alpha^{1/2}$
4	P4	Power law	$2/3\alpha^{-1/2}$	$\alpha^{3/2}$
5	R1	Zero-order (Polanyi-Winger equation)	1	α
6	R2	Phase-boundary controlled reaction (contracting area, <i>i.e.</i> , bidimensional shape)	$2(1 - \alpha)^{1/2}$	$[1 - (1 - \alpha)^{1/2}]$
7	R3	Phase-boundary controlled reaction (contracting volume, <i>i.e.</i> , tridimensional shape)	$3(1 - \alpha)^{2/3}$	$[1 - (1 - \alpha)^{1/3}]$
8	F1	First-order (Mampel)	$(1 - \alpha)$	$-\ln(1 - \alpha)$
9	F3/2	Three-halves order	$(1 - \alpha)^{3/2}$	$2[(1 - \alpha)^{-1/2} - 1]$
10	F2	Second-order	$(1 - \alpha)^2$	$(1 - \alpha)^{-1} - 1$
11	F3	Third-order	$(1 - \alpha)^3$	$(1/2)[(1 - \alpha)^{-2} - 1]$
12	A3/2	Avrami-Erof'eev (n = 1.5)	$(3/2)(1 - \alpha)[- \ln(1 - \alpha)]^{1/3}$	$[- \ln(1 - \alpha)]^{2/3}$
13	A2	Avrami-Erof'eev (n = 2)	$2(1 - \alpha)[- \ln(1 - \alpha)]^{1/2}$	$[- \ln(1 - \alpha)]^{1/2}$
14	A3	Avrami-Erof'eev (n = 3)	$3(1 - \alpha)[- \ln(1 - \alpha)]^{2/3}$	$[- \ln(1 - \alpha)]^{1/3}$
15	A4	Avrami-Erof'eev (n = 4)	$4(1 - \alpha)[- \ln(1 - \alpha)]^{3/4}$	$[- \ln(1 - \alpha)]^{1/4}$
16	D1	One-dimensional diffusion	$(1/2)\alpha^{-1}$	α^2
17	D2	Two-dimensional diffusion (bidimensional particle shape) Valensi equation	$1/[- \ln(1 - \alpha)]$	$(1 - \alpha)\ln(1 - \alpha) + \alpha$
18	D3	Three-dimensional diffusion (tridimensional particle shape) Jander equation	$3/2(1 - \alpha)^{2/3} [1 - (1 - \alpha)^{1/3}]^{-1}$	$[1 - (1 - \alpha)^{1/3}]^2$
19	D4	Three-dimensional diffusion (tridimensional particle shape) Ginstling-Brounshtein	$3/2[(1 - \alpha)^{1/3} - 1]^{-1}$	$(1 - 2\alpha/3) - (1 - \alpha)^{2/3}$

for that α regardless of the model.

Kissinger-Akahira-Sunose (KAS) method [20] is another integral isoconversional method. This method is based on the following equation:

$$\ln\left(\frac{\beta}{T^2}\right) = \ln\left(\frac{AR}{E_a g(\alpha)}\right) - \frac{E_a}{RT} \quad (6)$$

Activation energy can be calculated from the linear plot of the left side of the above equation vs. $1/T$.

The Kissinger method is a model free approach, though is not an isoconversional method. Kissinger method is a peak method based on the shift in the peak maximum with the heating rate. If the reaction is assumed to be first-order ($n = 1$), ($f(\alpha) = (1 - \alpha)$), then the equation is simplified to below equation [21]:

$$\ln\left(\frac{\beta}{T_p^2}\right) = \ln\left(\frac{AR}{E_a}\right) - \frac{E_a}{RT_p} \quad (7)$$

where E_a is the activation energy, T_p is temperature at which $d\alpha/dt$ is maximum, A is pre-exponential factor, and R is gas constant. The activation energy is determined from the slope of the linear plot of the left-hand side of the above equation vs. $1/T_p$. Also, pre-exponential factor can be determined from the intercept of the plot.

Model-fitting Methods

Model-fitting method can be used to determine the triple kinetic parameters (E_a , A and $f(\alpha)$) of a degradation process. E_a and A are achieved by fitting different reaction models to experimental data (α vs. T) for a chosen reaction model. The best known model-fitting methods are the Coats-Redfern (CR) and Kennedy-Clark (KC) methods.

The Coats-Redfern (CR) [22] method is based on the Eq. (6) in the following form:

$$\ln\left(\frac{g(\alpha)}{T^2}\right) = \ln\left(\frac{AR}{\beta E_a} \left[1 - \left(\frac{2RT^*}{E_a}\right)\right]\right) - \frac{E_a}{RT} \quad (8)$$

where T^* is the mean experimental temperature.

The Kennedy-Clark (KC) [23] method is given by the following expression:

$$\ln\left[\frac{\beta g(\alpha)}{T - T_0}\right] = \ln(A) - \frac{E_a}{RT} \quad (9)$$

where T_0 is the temperature at which the degradation process starts.

Average apparent activation energy and average pre-exponential factor can be obtained from the slope and the intercept of the linear plot of the left-hand side of the Eq. (8) and the Eq. (9) vs. $1/T$ for a heating rate and given reaction model listed in Table 1 [15]. The model giving the best linear fit is selected as the model of choice.

Master-plots

Several efforts have been made to determine the solid state reaction models by using the so-called "master-plot". Master-plots are reference theoretical curves depending on the reaction model, but generally independent of the degradation kinetic parameters. We can obtain the most probable model by comparison of the theoretical master-plots drawn by assuming various kinetic models with the experimental master-plot. Application of the master-plot method for thermal analysis data requires previously knowledge of the activation energy. By selecting a reference point at $\alpha = 0.5$, the following differential master equation is easily derived from the Eq. (3) [16]:

$$\frac{f(\alpha)}{f(0.5)} = \frac{\left(\frac{d\alpha}{dT}\right) \text{Exp}\left(\frac{E_a}{RT}\right)}{\left(\frac{d\alpha}{dT}\right)_{0.5} \text{Exp}\left(\frac{E_a}{RT_{0.5}}\right)} \quad (10)$$

where $(d\alpha/dt)_{0.5}$, $T_{0.5}$, and $f(0.5)$ are the reaction rate, the reaction temperature, and the differential function of the reaction model at $\alpha = 0.5$, respectively. The left-hand side of the Eq. (10) is a reduced theoretical curve and the right-hand side of the equation is associated with the reduced rate and can be obtained from the experimental data.

Critical Explosion and Self-accelerating Decomposition Temperatures

The critical temperature of thermal explosion (T_b) and self-accelerating decomposition temperature (T_{SADT}) are two significant parameters to evaluate the thermal stability of energetic materials. The critical temperature of thermal

explosion (T_b) was defined as the lowest temperature at which a specific charge might be heated without undergoing thermal runaway [10]. T_{SADT} and T_b were obtained by the Eqs. (12) and (13), respectively:

$$T_e = T_{e0} + a\beta_i + b\beta_i^2 \quad (i = 1 - 4) \quad (11)$$

$$T_{SADT} = T_{e0} \quad (12)$$

$$T_b = \frac{E_0 - \sqrt{E_a^2 - 4E_a RT_{e0}}}{2R} \quad (13)$$

where a and b are coefficients, R is the universal gas constant, β_i is heating rate, and E_a is the value of E obtained by the Kissinger method. T_{e0} is defined as onset temperature (T_e) corresponding to $\beta_i \rightarrow 0$ by the Eq. (11).

EXPERIMENTAL

Materials

Epoxy resins (Araldite LY 5052) and curing agent (Aradur LY 5052) (Huntsman Advanced Materials) were used as received. Ammonium perchlorate (99.0%, Fluka) with average particle size about 50 μm , Strontium nitrate, Magnesium-Aluminum powder (Merck Company) with average particle sizes about 200 μm were used directly without further purification.

Instruments

Simultaneous DSC/TGA of the samples was studied by STA instrument (METLER Toledo) at 5 K min^{-1} heating rate from ambient temperature to 1000 $^\circ\text{C}$, and DSC experiments were studied by DSC instrument (METLER Toledo) at heating rates 3, 5, 10 and 20 K min^{-1} from ambient temperature to 600 $^\circ\text{C}$ under nitrogen atmosphere (50 ml min^{-1}). These analyses were performed with about 5-7 mg of samples in platinum pans. Indium standard was used to calibrate the DSC temperature scale before the use.

Sample Preparation

We decided to prepare a mixture containing of Mg-Al, ammonium perchlorate (AP), strontium nitrate powder, and epoxy with 28, 28, 19, 10 and 15 mass ratio, respectively. Then, a required amount of AP, strontium nitrate, and Mg-Al powder were carefully mixed together, and the agitation

was continued until a homogenous mixture was obtained. A required amount of epoxy/hardener curing agent at stoichiometric ratio (40/100 mass ratio of curing agent/epoxy resin) was dissolved in acetone solvent (1:1 mass ratio). The mixture was added to the solution and inserted into a cylindrical container and the agitation was continued until a homogenous mixture was obtained. Ultimately, curing reaction was carried out two stages curing cycle: first step at 23 $^\circ\text{C}$ during 24 h and second one in an oven, at 50 $^\circ\text{C}$ during 15 h. This curing cycle was chosen according to processing manual published by the supplier. Then, the samples were removed from the containers and retained in a dried and inert environment.

RESULTS AND DISCUSSION

Analysis of TG/DSC Data

Simultaneous DSC/TGA curves for the energetic mixture were recorded under nitrogen atmosphere at 5 K min^{-1} heating rate (Fig. 1). Figure 1 shows that degradation temperature of the energetic mixture was initiated ($\alpha = 0.05$) at about 170 $^\circ\text{C}$. It can be seen from the TG curve that mass loss of the mixture continues up to 600 $^\circ\text{C}$, which is associated by a mass loss of about 40%, and then it starts increasing weight due to oxidation of magnesium [2].

DSC curve of the energetic mixture shows two exothermic and two endothermic peaks (Fig. 1). The main exothermic peak occurs during the mass loss. The first endothermic peak observed at about 650 $^\circ\text{C}$ is attributed to the melting point of Mg-Al [12], and the second endothermic peak observed at about 900 $^\circ\text{C}$ is attributed to the decomposition of strontium nitrate [24]. The exothermic peak observed at 825 $^\circ\text{C}$ has not been seen for the pure samples [1,24], then it may be attributed to the reaction among the decomposition products. Due to the weight increase during the thermal analysis of the energetic mixture, we decided to study the degradation process of the mixture using DSC curves. Then, DSC curves of the mixture (2-3 mg weight samples) were recorded at 3, 5, 10 and 20 K min^{-1} heating rates from ambient temperature to 600 $^\circ\text{C}$ under nitrogen atmosphere to study the main exothermic peak (Fig. 2).

According to the obtained results at different heating

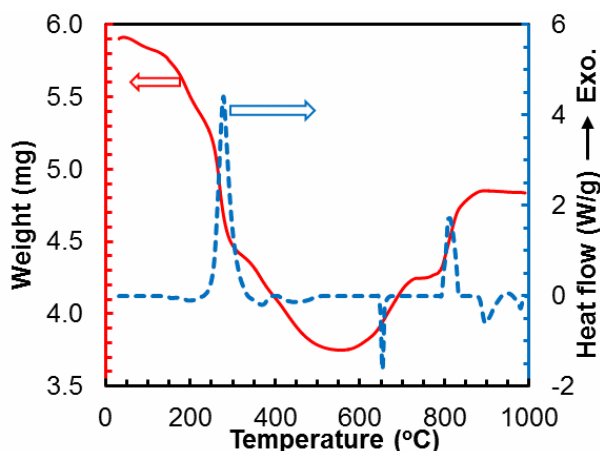


Fig. 1. DSC/TGA curve of the energetic mixture under nitrogen atmosphere at 10 K min⁻¹ heating rate.

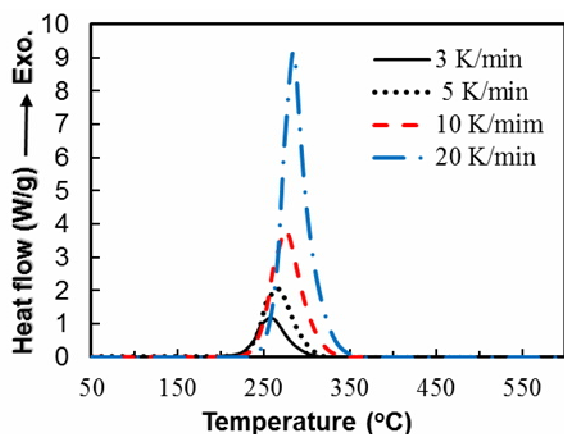


Fig. 2. DSC curves of the energetic mixture under nitrogen atmosphere at 3, 5, 10 and 20 K min⁻¹ heating rates.

ates, the values of characteristic temperatures (T_{onset} , T_{peak}) of DSC curves shift to higher temperatures with increasing heating rate, as expected (Fig. 2). Table 2 represents the characteristic temperatures and area under peak of the mixture at different heating rates. It can be found that area under the peak increases with increasing heating rate.

Figure 3 shows the variation of conversion with temperature for degradation of the mixture at different heating rates. It was found that the conversional curve shifts towards a higher temperature range with increasing the heating rate, meaning that increased degradation process of

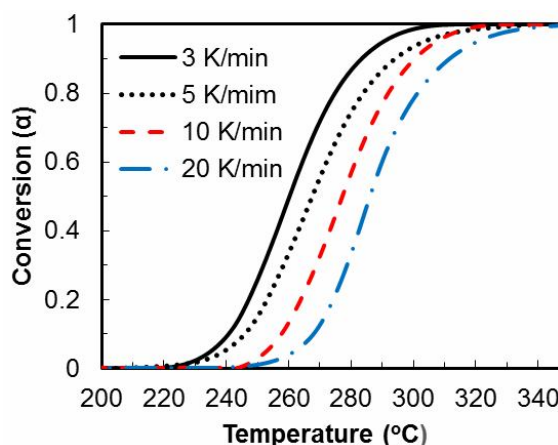


Fig. 3. Variation of conversion as a function of temperature for the energetic mixture under nitrogen atmosphere at different heating rates.

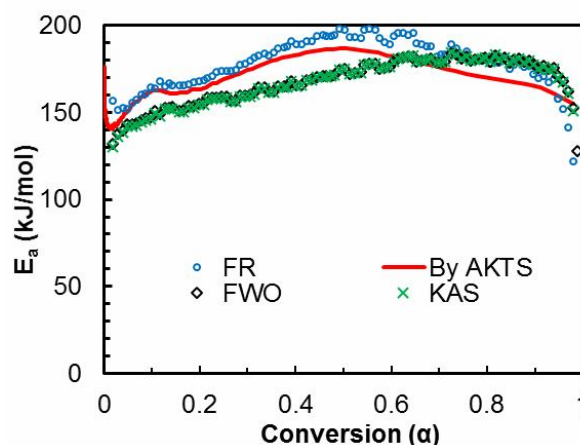


Fig. 4. Variation of degradation activation energy for the energetic mixture calculated by FR, FWO, KAS and AKTS software as a function conversion.

the energetic mixture will occur at a higher temperature.

Determination of Activation Energy

The dependence of E_a on α for the mixture was calculated using FWO, KAS, Friedman methods and by the AKTS software package. According to the recommendations of the International Confederation for Thermal Analysis and Calorimetry (ICTAC) [25], the E_a

Table 2. Characteristic Temperatures and Area under Peak of the Energetic Mixture at Different Heating Rates

β (K min ⁻¹)	T _{onset} (°C)	T _p (°C)	Peak area (J g ⁻¹)
3	233.5	257.1	837
5	239.0	265.8	954
10	247.0	275.4	1781
20	261.2	284.1	2491

Table 3. Triplet Kinetic Parameters Determined by Coats-Redfern and Kennedy-Clark Methods (Model-fitting) in the Range $\alpha = 0.10-0.90$ for the Energetic Mixture at 5 k min⁻¹ Heating Rate

Model	CR Method			KC Method		
	r ²	E _a	ln	r ²	E _a	lnA
P1	0.954	123.8	20.39	0.999	-30.0	13.11
P2	0.856	25.4	-1.26	0.976	-21.4	11.27
P3	0.882	42.6	2.74	0.196	-4.2	-7.60
P4	0.908	145.9	25.87	0.863	99.1	14.48
R1	0.902	94.3	14.43	0.797	47.5	3.44
R2	0.943	115.6	18.85	0.931	68.8	7.67
R3	0.954	123.8	20.39	0.937	77	9.15
F1	0.974	141.9	25.78	0.971	95.1	14.42
F1.5	0.991	173.4	33.2	0.995	126.6	21.65
F2	0.999	209.8	41.74	1	163.1	30
F3	0.997	294.9	61.54	0.991	248.1	49.48
A1.5	0.971	91.6	14.36	0.964	44.8	3.4
A2	0.969	66.4	8.58	0.944	19.6	-2.11
A3	0.964	41.3	2.69	0.963	-5.5	-7.62
A4	0.954	28.7	-0.29	0.994	-18.1	-10.37
D1	0.91	197.6	37.2	0.883	150.8	25.52
D2	0.933	223.3	42.57	0.919	176.5	30.77
D3	0.958	256.6	48.87	0.952	209.8	36.94
D4	0.942	234.2	43.63	0.932	187.4	31.79

values were determined in a wide range of $\alpha = 0.05 - 0.95$ with a step of 0.01 to report the resulting dependency of E_a vs. α . The variation of E_a on α , for degradation of the mixture has been shown in Fig. 4. The variation in E_a with α has been found nearly analogous in both FR and AKTS and in both FWO and KAS cases (Fig. 4). Also, there is a difference between E_a calculated by Friedman (a differential isoconversional method) and FWO, KAS (integral isoconversional methods). It is due to the way in which the relations forming the basis of the integral methods are derived. Figure 4 shows a nearly constant E_a in the range of $\alpha = 0.10 - 0.90$ for degradation of the mixture (average value is $E_a = 155 \pm 15 \text{ kJ mol}^{-1}$ for FR, KAS, and FWO). This is an advantage for a propellant, then it is possible to determine the most probable kinetic reaction model by model-fitting methods in this α range.

Xiaoli K. *et al.* [12] determined kinetic parameters of KClO_4/Mg (59/41 mass ratio) pyrotechnic mixture using the Kissinger method based on the DSC data of different heating rates (5, 15 and 20 K min^{-1}). The values of E_a and $\ln A$ for the ignition process were $153.6 \text{ kJ mol}^{-1}$, 21.50 s^{-1} , respectively.

Finding Triplet Kinetic Parameters

Activation energy, pre exponential factor and corresponding correlation coefficient (r^2) for different reaction models were determined at different heating rates by the Coats-Redfern (CR) and Kennedy-Clark (KC) model-fitting methods. Table 3 lists the obtained results at 5 K min^{-1} for degradation process of the mixture.

It can be found from the results presented in Table 3 that, the values of kinetic parameters ($\ln A$, E_a) strongly depend on the reaction model, but F type (reaction order mechanism, $f(\alpha) = (1 - \alpha)^n$) reaction models (specially F2 model, $f(\alpha) = (1 - \alpha)^2$) have the highest correlation coefficient in both CR and KC methods. In addition, activation energy obtained by the F1.5 (CR method) and F2 (KC method) models are close to that calculated by the model-free methods ($155 \pm 15 \text{ kJ mol}^{-1}$). Then, it seems that F type reaction models are the most suitable kinetic reaction model for degradation of the energetic mixture.

Confirmation of Reaction Model

Differential master-plot method was used to confirm the

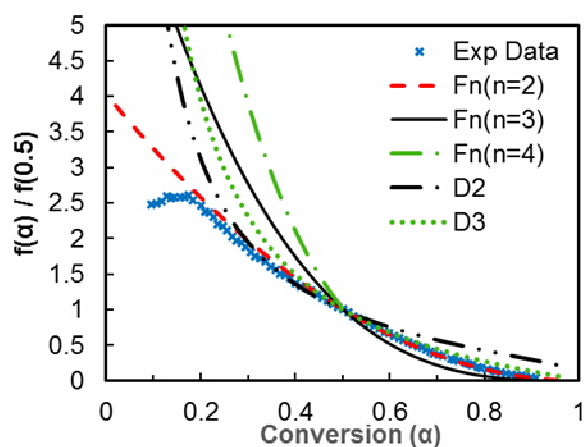


Fig. 5. Differential theoretical and experimental master-plot ($f(\alpha)/f(0.5)$) as a function of conversion for degradation of the energetic mixture.

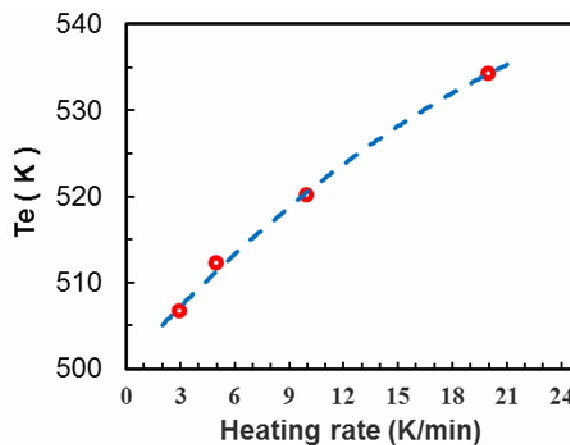


Fig. 6. Variation of onset temperature as a function of heating rate for the energetic mixture.

suggested reaction model according to the Eq. (10). Figure 5 shows the master plots of $f(\alpha)/f(0.5)$ vs. α for D2, D3, F2, F3 and F4 theoretical reaction models and experimental master plots for the degradation of the mixture at 5 K min^{-1} heating rate. Comparison of the experimental master plots with theoretical ones indicates that the thermal degradation process of the energetic mixture can be most probably described by F2 model (reaction order mechanism, $f(\alpha) = (1 - \alpha)^2$), in the range $\alpha = 0.2 - 0.90$. Investigation of the

experimental data at other considered heating rates shows that the degradation kinetic mechanism of the energetic mixture is constant at all heating rates for the same α range.

Critical Ignition Temperature

Figure 6 represents the variation of onset temperature *vs.* the heating rate for the energetic mixture. According to the Eq. (11), T_{e0} was obtained from the intercept of the fitted second-order equation with r^2 (correlation coefficient) above 0.97. The obtained value of T_{SADT} or T_{e0} is 227.4 °C. Peak temperatures of DSC curves at different heating rates were used to evaluate the activation energy by the Kissinger method (Eq. (6)). The calculated values of $\ln A$ and E_a of the mixture, according to the Kissinger method, are 23.9 1 s^{-1} and 155 kJ mol^{-1} , respectively. The E_a values calculated by the Kissinger method is equal to the E_a value calculated by the isoconversional methods. The critical temperature of thermal explosion (T_b) of the energetic mixture was calculated according to the Eq. (13) using the Kissinger activation energy. The obtained value of T_b is 241.7 °C for the mixture.

CONCLUSIONS

Non-isothermal DSC/TGA experiments of a fuel-rich mixture containing Mg/Al/AP/strontium nitrate/epoxy (28/28/19/10/15) were performed under nitrogen atmosphere conditions at different heating rates. The weight loss was initiated at 170 °C and showed a main exothermic peak at about 239 °C. It also started increasing weight up to 600 °C due to oxidation of magnesium. Variation of the activation energy curve of the energetic mixture *vs.* conversion showed a nearly smooth behavior (average value was $E_a = 155 \pm 15 \text{ kJ mol}^{-1}$ for the FR, KAS, and FWO methods), which was confirmed by the AKTS software package. The calculated values of $\ln A$ and E_a of the energetic mixture, according to the Kissinger method, were 23.9 1 s^{-1} and 155 kJ mol^{-1} , respectively. Degradation reaction mechanism of the mixture obeyed from F2 model, which was confirmed by differential master-plot method. The critical temperature of thermal explosion (T_b) and self-accelerating decomposition temperature (T_{SADT}) of the mixture were 227.4 °C and 241.7 °C, respectively.

REFERENCES

- [1] Fathollahi, M.; Behnejad, H., A comparative study of thermal behaviors and kinetics analysis of the pyrotechnic compositions containing Mg and Al. *J. Therm. Anal. Calorim.*, **2015**, *120*, 1483-1492, DOI: 10.1007/s10973-015-4433-3.
- [2] Huang, H. -T.; Zou, M. -S.; Guo, X. -Y.; Yang, R. -J.; Li, Y. -K., Reactions characteristics of different powders in heated steam. *Combust. Sci. Technol.*, **2015**, *187*, 797-806, DOI: 10.1080/00102202.2014.973950.
- [3] Jain, S., Solid propellant binders. *J. Sci. Ind. Res.*, **2002**, *61*, 899-911.
- [4] Zhu, Y. -L.; Huang, H.; Ren, H.; Jiao, Q. -J., Kinetics of thermal decomposition of ammonium perchlorate by TG/DSC-MS-FTIR. *J. Energ. Mater.*, **2014**, *32*, 16-26, DOI: 10.1080/07370652.2012.725453.
- [5] Wang, Q.; Wang, L.; Zhang, X.; Mi, Z., Thermal stability and kinetic of decomposition of nitrated HTPB. *J. Hazard. Mater.*, **2009**, *172*, 1659-1664, DOI: 10.1016/j.jhazmat.2009.08.040.
- [6] Huang, H. T.; Zou, M. S.; Guo, X. Y.; Yang, R. J.; Zhang, P., Analysis of the solid combustion products of a Mg-based fuel-rich propellant used for water ramjet engines. *Propellants Explos. Pyrotech.*, **2012**, *37*, 407-412, DOI: 10.1002/prop.201100127.
- [7] Sippel, T. R.; Son, S. F.; Groven, L. J., Aluminum agglomeration reduction in a composite propellant using tailored Al/PTFE particles. *Combust. Flame.*, **2014**, *161*, 311-321, DOI: 10.1016/j.combustflame.2013.08.009.
- [8] Ghassemi, H.; Fasih, H. F., Propulsive characteristics of metal fuel-rich pyrotechnics in hydro-reactive motors. *Aero. Sci. Tech.*, **2013**, *28*, 1-8, DOI: 10.1016/j.ast.2012.08.011.
- [9] Sovizi, M.; Anbaz, K., Kinetic investigation on thermal decomposition of organophosphorous compounds: N,N-dimethyl-N',N'-diphenylphosphorodihydrazidic and diphenyl amidophosphate. *J. Therm. Anal. Calorim.*, **2009**, *99*, 593-598, DOI: 10.1007/s10973-009-0502-9.
- [10] Sovizi, M.; Hajimirsadeghi, S.; Naderizadeh, B., Effect of particle size on thermal decomposition of

- nitrocellulose. *J. Hazard. Mater.*, **2009**, *168*, 1134-1139, DOI: 10.1016/j.jhazmat.2009.02.146.
- [11] Boldyrev, V., Thermal decomposition of ammonium perchlorate. *Thermochim. Acta.*, **2006**, *443*, 1-36, DOI: 10.1016/j.tca.2005.11.038.
- [12] Kang, X.; Zhang, J.; Zhang, Q.; Du, K.; Tang, Y., Studies on ignition and afterburning processes of KClO₄/Mg pyrotechnics heated in air. *J. Therm. Anal. Calorim.*, **2011**, *109*, 1333-1340, DOI: 10.1007/s10973-011-1991-x.
- [13] AKTS-Thermokinetics Software, Advanced Kinetics and Technology Solutions, <http://www.akts.com>.
- [14] Sovizi, M. R.; Fakhrpour, G.; Bagheri, S.; Bardajee, G. R., Non-isothermal dehydration kinetic study of a new swollen biopolymer silver nanocomposite hydrogel. *J. Therm. Anal. Calorim.*, **2015**, *121*, 1383-1391, DOI: 10.1007/s10973-015-4639-4.
- [15] Janković, B.; Adnadević, B.; Jovanović, J., Application of model-fitting and model-free kinetics to the study of non-isothermal dehydration of equilibrium swollen poly (acrylic acid) hydrogel: thermogravimetric analysis. *Thermochim. Acta.*, **2007**, *452*, 106-115, DOI: 10.1016/j.tca.2006.07.022.
- [16] Fakhrpour, G.; Bagheri, S.; Golriz, M.; Shekari, M.; Omrani, A.; Shameli, A., Degradation kinetics of PET/PEN blend nanocomposites using differential isoconversional and differential master plot approaches. *J. Therm. Anal. Calorim.*, **2016**, *124*, 917-924, DOI: 10.1007/s10973-10015-15024-z.
- [17] Friedman, H. L., editor. Kinetics of thermal degradation of char-forming plastics from thermogravimetry. Application to a phenolic plastic. *J. Polym. Sci., Part C: Polym. Symp.*; **1964**: Wiley Online Library, DOI: 10.1002/polc.5070060121.
- [18] Ozawa, T., Kinetics in differential thermal analysis. *Bull. Chem. Soc. Jpn.*, **1965**, *38*, 1881-1886.
- [19] Flynn, J. H.; Wall, L. A., General treatment of the thermogravimetry of polymers. *J. Res. Nat. Bur. Stand.*, **1966**, *70*, 487-523.
- [20] Akahira, T.; Sunose, T., Method of determining activation deterioration constant of electrical insulating materials. *Res. Rep. Chiba. Inst. Technol. (Sci. Technol.)*, **1971**, *16*, 22-31.
- [21] Blaine, R. L.; Kissinger, H. E., Homer Kissinger and the Kissinger equation. *Thermochim. Acta.*, **2012**, *540*, 1-6, DOI: 10.1002/prop.201100127.
- [22] Doyle, C. D., Series approximations to the equation of thermogravimetric data., **1965**, p. 290-291, DOI: 10.1038/207290a0.
- [23] Kennedy, J.; Clark, S., A new method for the analysis of non-isothermal DSC and diffraction data. *Thermochim. Acta.*, **1997**, *307*, 27-35, DOI: 10.1016/S0040-6031(96)02962-0.
- [24] Culas, S.; Samuel, J., γ -Irradiation effects on the non-isothermal decomposition of strontium nitrate by model-free and model-fitting methods. *Radiat. Phys. Chem.*, **2013**, *86*, 90-95, DOI: 10.1016/j.radphyschem.2013.01.042.
- [25] Vyazovkin, S.; Burnham, A. K.; Criado, J. M.; Pérez-Maqueda, L. A.; Popescu, C.; Sbirrazzuoli, N., ICTAC kinetics committee recommendations for performing kinetic computations on thermal analysis data. *Thermochim. Acta.*, **2011**, *520*, 1-19, DOI: 10.1016/j.tca.2011.03.034.